



ENSO flavors in a tree-ring $\delta^{18}\text{O}$ record of *Tectona grandis* from Indonesia

K. Schollaen^{1,2}, C. Karamperidou³, P. Krusic^{4,5}, E. Cook⁶, and G. Helle¹

¹GFZ – German Research Centre for Geosciences, Section 5.2 Climate Dynamics and Landscape Evolution, Potsdam, Germany

²Alfred Wegener Institute Helmholtz Centre for Polar and Marine Research, Potsdam, Germany

³Department of Atmospheric Sciences, University of Hawaii at Manoa, Honolulu, Hawaii, USA

⁴Navarino Environmental Obs. Messinia, Greece

⁵Department of Physical Geography and Quaternary Geology, Stockholm University, Stockholm, Sweden

⁶Tree Ring Laboratory, Lamont-Doherty Earth Observatory, Columbia University, USA

Correspondence to: K. Schollaen (karina.schollaen@gmail.com)

Received: 29 August 2014 – Published in Clim. Past Discuss.: 2 October 2014

Revised: 21 August 2015 – Accepted: 23 September 2015 – Published: 8 October 2015

Abstract. Indonesia's climate is dominated by the equatorial monsoon system, and has been linked to El Niño-Southern Oscillation (ENSO) events that often result in extensive droughts and floods over the Indonesian archipelago. In this study we investigate ENSO-related signals in a tree-ring $\delta^{18}\text{O}$ record (1900–2007) of Javanese teak. Our results reveal a clear influence of Warm Pool (central Pacific) El Niño events on Javanese tree-ring $\delta^{18}\text{O}$, and no clear signal of Cold Tongue (eastern Pacific) El Niño events. These results are consistent with the distinct impacts of the two ENSO flavors on Javanese precipitation, and illustrate the importance of considering ENSO flavors when interpreting palaeoclimate proxy records in the tropics, as well as the potential of palaeoclimate proxy records from appropriately selected tropical regions for reconstructing past variability of ENSO flavors.

1 Introduction

The tropical warm pool surrounding the Indonesian maritime continent (IMC) is a region of homogenous sea surface temperatures where atmospheric deep convection occurs, and plays a key role in the regulation of the global tropical climate (Clement et al., 2005; Pierrehumbert, 1995).

Indonesia's regional climate is governed by the Australian-Indonesian Monsoon (Wheeler and McBride, 2005) and the

associated seasonal movement of the Inter Tropical Convergence Zone (ITCZ). Variations of the equatorial monsoon system significantly impact the livelihood of over 230 million people living in the world's fourth most populated country.

The El Niño-Southern Oscillation (ENSO) phenomenon contributes to the rainfall pattern of the IMC and has been thought to interact with the monsoons (e.g., Hendon, 2003; Lau and Nath, 2000). Recent studies have drawn attention to the existence of more than one variant or *flavors* of El Niño (the warm phase of ENSO) (Ashok et al., 2007; Kug et al., 2009; Larkin and Harrison, 2005; Ren and Jin, 2011; Takahashi et al., 2011). The canonical El Niño (Sarachik and Cane, 2010), also referred to as eastern Pacific (EP) El Niño (Kao and Yu, 2009) or Cold Tongue El Niño (Kug et al., 2009; Ren and Jin, 2011), exhibits SST anomalies localized in the eastern equatorial Pacific. The El Niño variant with maximum SST anomalies located in the central equatorial Pacific is referred to as the central Pacific (CP) El Niño (Kao and Yu, 2009), Warm Pool (WP) El Niño (Kug et al., 2009; Ren and Jin, 2011), date line El Niño (Larkin and Harrison, 2005) or El Niño Modoki (Ashok et al., 2007; Takahashi et al., 2011). In this study we use the terms Cold Tongue (CT), and Warm Pool (WP) El Niño (Ren and Jin, 2011) to describe these two ENSO flavors.

Identifying the mechanisms responsible for the CT and WP ENSO flavors is an active field of research. At present, there is no consensus on whether a reported increase in

the frequency and intensity of WP ENSO events in recent decades (Ashok et al., 2007; Kao and Yu, 2009; Kug et al., 2009; Lee and McPhaden, 2010) is a result of anthropogenic greenhouse gas forcing (Yeh et al., 2009), or natural variability (McPhaden et al., 2011; Newman et al., 2011). In addition, the simulation of ENSO flavors in Global Climate Models (GCMs) is still subject to limitations in our understanding of the phenomenon. Consequently, there is much uncertainty about whether ENSO activity will be enhanced or damped in the future, or if the relative frequency of ENSO flavors will change (Collins et al., 2010). Long records of ENSO activity are essential for identifying trends and multidecadal changes in the patterns of sea surface temperature associated with ENSO, making palaeoclimate reconstructions particularly attractive for shedding light onto the past and future of ENSO flavors.

Recent research on ENSO-proxy teleconnections recommends, that when interpreting proxy data, differences in the influence of the two ENSO flavors on SST, precipitation and salinity should be taken into account (Karamperidou et al., 2015). Certain regions like Java lie in key locations where interannual precipitation variability is significantly correlated to one ENSO flavor but not the other (see Fig. 1). Thus, long-term rainfall proxies from Java can be useful for distinguishing between ENSO flavors, and for studying their relation to monsoon variability.

Over the last decade there have been several attempts to reconstruct continuous time series of ENSO variability using different proxy archives such as corals (e.g., Abram et al., 2008; Charles et al., 2003; Cobb et al., 2013; Evans et al., 2002; Linsley et al., 2004; Pfeiffer et al., 2009; Quinn et al., 2006; Wilson et al., 2006), tree-ring widths (e.g., D'Arrigo et al., 2005; Fowler et al., 2012; Stahle et al., 1998) or tree-ring stable isotopes (Sano et al., 2012). Furthermore, several multi-proxy reconstructions of ENSO variability are available (e.g., Braganza et al., 2009; D'Arrigo et al., 2006; Emile-Geay et al., 2013; Mann et al., 2000; Wilson et al., 2010). However, many of these reconstructions are based on extratropical proxy records, particularly from tree-ring widths, and thus do not represent ENSO activity directly.

Tree-ring stable isotopes often provide additional climate information where the more commonly used tree-ring proxies (e.g., ring width and maximum latewood density) do not, or where the teleconnection signal is weak. In tropical regions, oxygen isotope data from tree rings ($\delta^{18}\text{O}_{\text{TR}}$) are often more sensitive to precipitation than ring width (e.g., Brien et al., 2012; Schollaen et al., 2013). $\delta^{18}\text{O}_{\text{TR}}$ data are primarily controlled by the isotopic composition of precipitation, i.e., the source water, and relative humidity (e.g., Barbour, 2007; McCarroll and Loader, 2004). The isotopic composition of precipitation ($\delta^{18}\text{O}_{\text{Pre}}$) depends on a number of factors, the so-called “kinetic isotope effects” (Araguás-Araguás et al., 2000). One of these effects, “the amount effect”, is the inverse correlation between rainfall amount and $\delta^{18}\text{O}_{\text{Pre}}$ values, and a crucial driver in determining $\delta^{18}\text{O}_{\text{Pre}}$

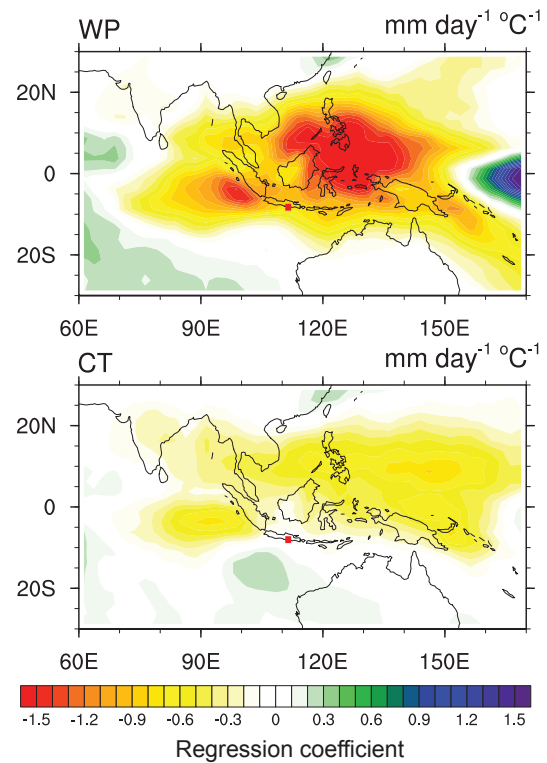


Figure 1. Regression coefficients ($\text{mm day}^{-1} \text{ } ^\circ\text{C}^{-1}$) of monthly precipitation on the Warm Pool (WP) and the Cold Tongue (CT) ENSO index. The two indices are computed as per Ren and Jin (2011) (Eq. 1). Precipitation data are from the GPCP (Adler et al., 2003), for the period 1987–2010. The tree-ring site is marked with a red square.

values in the tropics (e.g., Brien et al., 2012; Zhu et al., 2012). Thus $\delta^{18}\text{O}_{\text{TR}}$ records offer a promising approach to examine monsoon activity, and large-scale climate variations such as ENSO.

In previous studies we investigated relationships between seasonal rainfall variability and tree-ring stable isotope records from Javanese teak trees on inter- to intra-annual timescales (Schollaen et al., 2013, 2014). In this study we explore the signal strength of ENSO flavors in our annually resolved $\delta^{18}\text{O}_{\text{TR}}$ record from Java, the only well replicated, centennial $\delta^{18}\text{O}$ record from Javanese teak in existence. We place particular emphasis on the time stability of the teleconnected $\delta^{18}\text{O}/\text{ENSO}$ relationship. To the best of our knowledge this is the first time the relationship between tree-ring proxies and the two ENSO flavors has been tested. We find a unique WP El Niño signal in the $\delta^{18}\text{O}_{\text{TR}}$ record from Java, supporting the notion that proxies from carefully selected regions are valuable for answering questions of past and present ENSO variability, and for constructing reliable ENSO reconstructions.

2 Data and methods

2.1 Proxy data and site description

We use a tree-ring $\delta^{18}\text{O}$ chronology from a lowland rainforest in the eastern part of Central Java, Indonesia ($07^{\circ}52' \text{S}$, $111^{\circ}11' \text{E}$; 380 m a.s.l.), spanning the period 1900–2007. The $\delta^{18}\text{O}_{\text{TR}}$ record is built from resin-extracted wood of seven teak (*Tectona grandis*) trees, collected from the Donoloyo Cagar Alam (site DNLY in D'Arrigo et al., 2006) shown as green lines in Fig. 2. The according TRW chronology dates back to AD 1714. This $\delta^{18}\text{O}_{\text{TR}}$ chronology and its dendroclimatological potential as a rainfall indicator has been described in detail in Schollaen et al. (2013). Indonesia receives significant rainfall year-round but experiences a distinct wet and dry season. The wet season (approx. October/November to April/May) coincides with movement of the Inter-Tropical Convergence Zone to the Southern Hemisphere, while the dry season (June to September) corresponds with a predominance of dry southeasterly winds from Australia (Aldrian et al., 2007). The isotopic composition of precipitation ($\delta^{18}\text{O}_{\text{Pre}}$) over Java shows that distinct seasonal changes are linked to rainfall amount resulting in high $\delta^{18}\text{O}_{\text{Pre}}$ values during the dry season, and low $\delta^{18}\text{O}_{\text{Pre}}$ values during the rainy season (Fig. 5b of Schollaen et al., 2014). Instrumental records (e.g., Aldrian and Susanto, 2003; Allan, 2000; Haylock and McBride, 2001) and reanalysis products (Aldrian et al., 2007; Jourdain et al., 2013) show rainfall anomalies in Indonesia are affected by ENSO: during a warm ENSO phase (El Niño events) the tropospheric air flow (Walker Circulation) weakens and the Indonesian low pressure system migrates eastward into the tropical Pacific, resulting in drought over much of the country. Conversely, a cold ENSO phase (La Niña events) brings excess rain to the region (Sarachik and Cane, 2010). Several analyses of Indonesian rain gauge data show that Indonesian rainfall is poorly correlated with ENSO events during the wet monsoon season, but reveal highest coherence during the dry season and transition months prior to the wet season (June to November) (Haylock and McBride, 2001; Hendon, 2003). However, taking the IMC and surrounding oceanic rainfall into account, rainfall during the wet season is also related to ENSO (Fig. 8a of Jourdain et al., 2013).

In this study, we further show that precipitation anomalies in Java are sensitive to ENSO flavors. Figure 1 shows the relationship between precipitation data and the WP and CT ENSO indices (see Sect. 2.2 for definition of the indices) for the IMC and Pacific region. WP El Niños are associated with drought over Java (Fig. 1, upper panel), and have a strong influence on the Australian-Indonesian monsoon system (e.g., Kumar et al., 2006; Taschetto and England, 2009). On the other hand, Java lies on the nodal line of influence of CT El Niños (Fig. 1, lower panel), which makes it a key location for obtaining records able to distinguish between the two ENSO flavors. The average regression coefficient between monthly

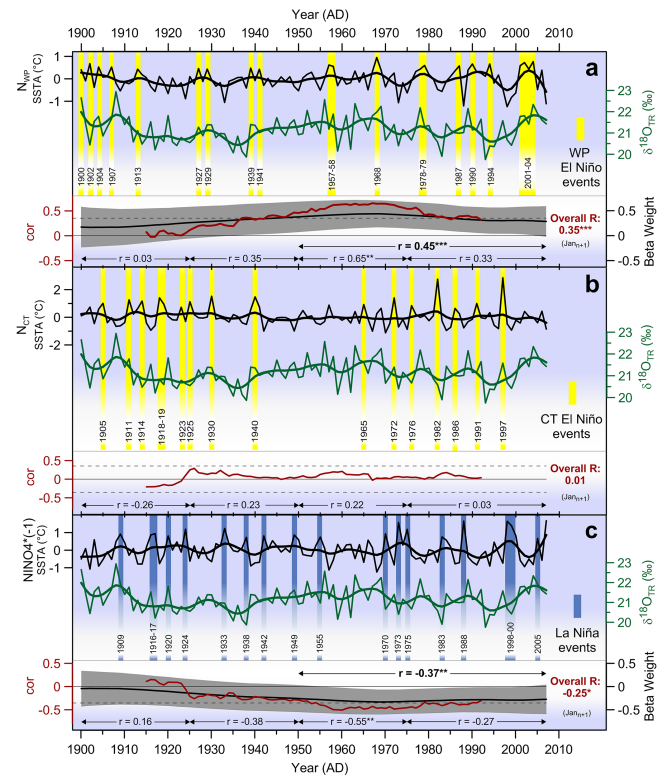


Figure 2. Time series of the $\delta^{18}\text{O}_{\text{TR}}$ chronology (green) and the January (Jan_{n+1}) indices of (a) Warm Pool ENSO (N_{WP}), (b) Cold Tongue ENSO (N_{CT}), and (c) negative NINO4 index ($\text{NINO4} \times (-1)$), used here as a La Niña index. The WP and CT ENSO indices are computed as per Ren and Jin (2011) (Eq. 1). Thick lines denote 10-year cubic smoothing spline. In the lower part of each figure the running 31-year correlation (red) is shown. Dashed horizontal line indicates the 95 % confidence level. Also shown are the results from a Kalman filter analysis (black line) used as a dynamic regression-modeling tool. Gray shading denotes ± 2 standard error limits of the beta weights. Where the limits do not cross zero, the regression relationship is considered statistically significant ($p = 95\%$). ENSO events based on classification of Table 1 are highlighted in yellow (El Niño) and blue (La Niña), respectively. (***) $p < 0.001$, (**) $p < 0.01$, (*) $p < 0.05$.

precipitation anomalies over Java and the WP ENSO index is $-0.83 \text{ mm day}^{-1}$, while for CT ENSO it is $-0.03 \text{ mm day}^{-1}$ (non-significant).

The growing season for teak in Central and Eastern Java occurs mostly during the wet season, from October to May (Coster, 1928, 1927; Geiger, 1915; Schollaen et al., 2013). In all subsequent analysis, we use the Southern Hemisphere convention, which assigns to each tree ring the year in which radial growth begins (Schulman, 1956). Thus lag-0 refers to the year n where tree growth starts: $\text{Oct}_n\text{--Sep}_{n+1}$. Lag-1 refers to $\text{Oct}_{n-1}\text{--Sep}_n$.

2.2 Definition of ENSO flavors

In the following, we use the global SST data set of Kaplan et al. (1998). To calculate indices for the two ENSO flavors we use the coordinate transform of the NINO3-NINO4 phase space proposed by Ren and Jin (2011) and shown in Eq. (1).

$$\begin{aligned} N_{CT} &= N_3 - \alpha N_4 \\ N_{WP} &= N_4 - \alpha N_3, \quad \alpha = \begin{cases} 2/5 & \text{if } N_3 \times N_4 > 0 \\ 0 & \text{otherwise} \end{cases} \end{aligned} \quad (1)$$

where N_{CT} , N_{WP} are the indices for CT and WP ENSO, and N_3 , N_4 are the NINO3 and NINO4 indices, i.e., the SST anomaly averaged over the regions $[5^\circ\text{N}–5^\circ\text{S}, 150–90^\circ\text{W}]$ and $[5^\circ\text{N}–5^\circ\text{S}, 160^\circ\text{E}–150^\circ\text{W}]$ respectively. The time series of the two indices N_{CT} , N_{WP} are shown in Fig. 2a and b (January values). When a Warm Pool event occurs (e.g., 1994–1995), SST anomalies are mostly concentrated in the NINO4 region, and therefore the N_{CT} index resulting from Eq. (1) is very small. In contrast, the N_{WP} index, which is dominated by the NINO4 anomalies, is large and, thus, the event is classified as a Warm Pool event. The opposite occurs during large Cold Tongue events (e.g., 1976–1977, 1982–1983, and 1997–1998): NINO3 anomalies dominate NINO4, and thus the N_{WP} index is very small compared to N_{CT} , and the event is classified by Eq. (1) as a Cold Tongue event. As shown in detail in Ren and Jin (2011), the two indices are able to capture the SST anomaly patterns that characterize the two ENSO flavors, as well as their variability in the 20th century. No significant differences were found when using alternative indices (Ashok et al., 2007; Takahashi et al., 2011) for calculating ENSO flavors (not shown here). Distinguishing between the two corresponding types of La Niña events, as advocated by Kao and Yu (2009) and Ashok and Yamagata (2009), may not be necessary because the SST and precipitation patterns of the two La Niña types are not very distinctive (Kug and Ham, 2011) and the SST anomalies during La Niña events generally tend to propagate westward. Therefore a single index (NINO4) suffices to capture La Niña events, as shown in Fig. 2c, and a coordinate transform of two indices (as in Eq. 1 above) is not necessary.

For subsequent analyses we use the January (Jan_{n+1}) indices for the ENSO flavors for the timespan 1900–2007. We focus on the month of January as that represents the month with highest precipitation during the rainy season at the study site. Here, our $\delta^{18}\text{O}_{\text{TR}}$ record correlates the best with regional rainfall data (Schollaen et al., 2013). We classify each year as CT, or WP when N_{CT} , or N_{WP} are greater than one standard deviation of the respective monthly index. We classify a year as La Niña (LN) when NINO4 is negative by less than one standard deviation of the monthly NINO4 index. Table 1 shows the list of years classified as CT, WP, and LN according to the above criteria.

2.3 ENSO signal assessment

To assess the long-term temporal stability of the ENSO signal, running 31-year correlations were calculated between the $\delta^{18}\text{O}_{\text{TR}}$ record and the varying ENSO flavors. A Kalman filter analysis was also used as a time-dependent regression-modeling tool to test the temporal stability of the relationship between the $\delta^{18}\text{O}_{\text{TR}}$ record and the two ENSO flavors. In contrast to the running correlation procedure, the Kalman filter method uses maximum likelihood estimation to objectively test for the identification of time-dependence between predictor and predicted variables (see Visser and Molenaar, 1988 for details, and Cook et al., 2002, 2013 or Wilson et al., 2013 for examples).

Furthermore, probability density functions of the correlation between $\delta^{18}\text{O}_{\text{TR}}$ variability and the different ENSO phases (WP, CT and LN), as well as during neutral conditions, were calculated. We classify neutral conditions when CT or WP are not greater than one standard deviation of the respective monthly index and when LN is negative by more than one standard deviation of the monthly NINO4 index. Finally, the spectral properties of the $\delta^{18}\text{O}_{\text{TR}}$ proxy time series were analyzed (Schulz and Mudelsee, 2002) and wavelet coherency analysis performed (Grinsted et al., 2004; Torrence and Compo, 1998).

3 Results

Monthly and seasonal correlations between the Javanese $\delta^{18}\text{O}_{\text{TR}}$ record (Fig. 2, green line in all plots) and ENSO flavors (see Sect. 2.2) were computed for both the concurrent year (lag-0) and the year prior to tree growth (lag-1) (Table 2). Statistically significant (95 % level or higher) positive correlations were found between WP El Niño and the concurrent rainy season ($\text{Oct}_n\text{–May}_{n+1}$, $r = 0.26$). Correlations are strongest with Jan_{n+1} ($r = 0.35$), the period of maximum rainy season precipitation. Furthermore, there is a significant correlation with lag-1 January precipitation (Jan_n , $r = 0.22$), indicating a WP El Niño influence on tree growth in the following year. Statistically significant negative correlations were found for La Niña events in January (Jan_{n+1} , $r = -0.25$) (Table 2). No positive correlation was found between the tree-ring proxy and the CT ENSO index (Table 2). As noted, the CT ENSO flavor has a weaker influence over Java (Fig. 1), therefore we expected the lag-0 correlation to be insignificant. For reference, we also present the correlation with the standard ENSO index NINO3.4, which shows no significance.

Although the $\delta^{18}\text{O}_{\text{TR}}$ record correlates significantly ($p < 0.05$) with ENSO flavors, the response is not stationary. Figure 2 presents the running 31-year correlation and Kalman filter analysis between the varying ENSO flavors and the tree-ring proxy for the period of highest correlation (see Table 2). The teleconnection with Jan_{n+1} WP ENSO is strong and significantly positive from the 1950s until present,

Table 1. Classification into ENSO flavors and phase based on Jan_{n+1} values (see Sect. 2.2). Note the use of the Southern Hemisphere convention (Schulman, 1956), i.e., year n refers to Jan_{n+1} .

ENSO classification	Years										
WP	1900	1902	1904	1907	1913	1927	1929	1939	1941	1957	1958
	1968	1978	1979	1987	1990	1994	2001	2002	2003	2004	
CT	1905	1911	1914	1918	1919	1923	1925	1930	1940	1965	
	1976	1982	1986	1991	1997						
LN	1909	1916	1917	1920	1924	1933	1938	1942	1949	1955	1970
	1973	1975	1983	1988	1998	1999	2000	2005	2007		

Table 2. Correlation values between the annually resolved $\delta^{18}\text{O}_{\text{TR}}$ record and climate months of different ENSO flavors and the standard NINO3.4 and La Niña index ($\text{NINO4} \times (-1)$) for the period from the year prior to growth (lag-1) to the current year (lag-0) and seasonal means (calculated over the 1900–2007 period). (** $p < 0.001$, * $p < 0.01$, bold: $p < 0.05$).

Climate months lag1 lag0	WP El Niño	CT El Niño	NINO3.4	La Niña
Oct _{n-1} Oct _n	0.12 0.21	-0.18 -0.03	-0.10 0.08	0.00 -0.14
Nov _{n-1} Nov _n	0.17 0.17	-0.23 -0.01	-0.13 0.05	0.00 -0.12
Dec _{n-1} Dec _n	0.18 0.18	-0.20 0.04	-0.11 0.10	-0.01 -0.15
Jan _n Jan _{n+1}	0.22 0.35 **	-0.19 -0.01	-0.07 0.12	-0.06 -0.25 *
Feb _n Feb _{n+1}	0.15 0.29 *	-0.15 -0.06	-0.07 0.09	-0.05 -0.21
Mar _n Mar _{n+1}	0.05 0.21	-0.17 -0.12	-0.10 0.02	0.03 -0.12
Apr _n Apr _{n+1}	0.14 0.21	-0.21 -0.09	-0.12 0.01	-0.02 -0.15
May _n May _{n+1}	0.12 0.20	-0.14 -0.11	-0.06 -0.01	-0.03 -0.12
Jun _n Jun _{n+1}	0.14 0.08	-0.07 -0.06	0.00 -0.03	-0.08 -0.03
Jul _n Jul _{n+1}	0.12 0.16	-0.02 -0.08	0.05 -0.03	-0.09 -0.10
Aug _n Aug _{n+1}	0.11 0.10	-0.02 -0.07	0.07 -0.03	-0.10 -0.05
Sep _n Sep _{n+1}	0.17 0.01	-0.05 -0.05	0.03 -0.06	-0.11 0.02
peak wet season (Jan _{n+1})	0.35 **			-0.25 *
Dec _n -Feb _{n+1}	0.27 *			-0.21
wet season (Oct _n -May _{n+1})	0.26 *			

with running correlations reaching 0.6, and an r of 0.45 for AD 1950–2007 ($p < 0.001$) (Fig. 2a). However, before 1950 the correlation falls to zero, and even becomes negative. The Kalman filter time-varying regression coefficients (beta weights) follow the same trend as the correlation values and reinforce the time dependency of the teleconnection. From 1950 onwards, the lower limits do not cross zero, which means that the beta weights are considered statistically significant. However, the correlation weakens slightly again in the beginning of the 21st century. The relationship with Jan_{n+1} NINO4 (used here to primarily capture La Niña events) (Fig. 2c) is also time-dependent with weak correlations before 1950 and after 2000, but a significant negative relationship in the second half of the century with $r = -0.37$ ($p < 0.01$).

The fingerprints of the ENSO flavors in the $\delta^{18}\text{O}_{\text{TR}}$ record can be seen in the probability density function (PDF) of $\delta^{18}\text{O}_{\text{TR}}$ anomalies (Fig. 3) conditioned on ENSO phase. The $\delta^{18}\text{O}_{\text{TR}}$ probability mass for WP El Niño is skewed towards

positive anomalies associated with dry conditions. By contrast, the PDF for CT El Niño events exhibits bimodality with peaks in both positive and negative $\delta^{18}\text{O}_{\text{TR}}$ anomalies, suggesting this record is not a good proxy for CT El Niño variability.

To further investigate expressions of ENSO variability in the $\delta^{18}\text{O}_{\text{TR}}$ record we performed spectral analysis (Fig. 4a). Spectral analysis of the $\delta^{18}\text{O}_{\text{TR}}$ record reveals a broad peak at 2–4 years, falling within the classic ENSO bandwidth (Sarachik and Cane, 2010) as well as significant, decadal-to-multidecadal variability (12.5 years). Wavelet coherence analysis between the proxy record and the WP ENSO and CT ENSO index (Fig. 4b, c) indicates that the coherence varies in time across most spectral bands. The periods of greatest coherence in time occur on inter-annual timescales (2–4 years), again spanning the classic ENSO bandwidth. We found no significant coherence with CT ENSO index as expected.

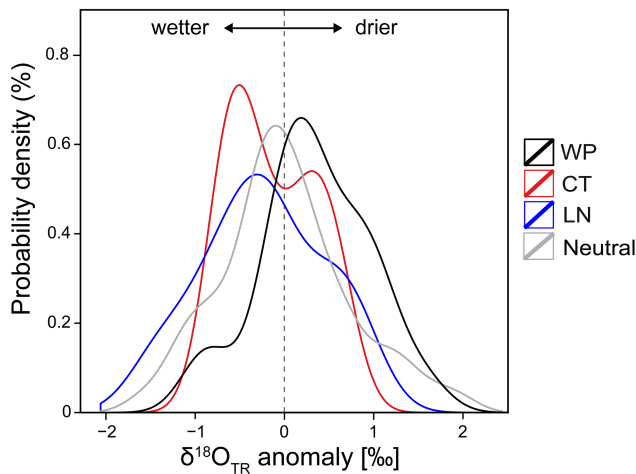


Figure 3. Probability density function of tree-ring $\delta^{18}\text{O}$ variability conditional on different ENSO phases: Warm Pool El Niño (WP, black line), Cold Tongue El Niño (CT, red line), La Niña (LN, blue line) and neutral conditions (gray line). For the construction of the PDF, we use January–February ($\text{Jan}_{n+1}\text{Feb}_{n+1}$) time-averaged values; the events considered for each conditional PDF are shown in Table 1.

4 Discussion

The positive correlation pattern between the $\delta^{18}\text{O}_{\text{TR}}$ record and the WP ENSO index, as well as the negative correlation with La Niña events, supports the conclusion in Schollaen et al. (2013) that the formation of annual $\delta^{18}\text{O}$ in Javanese teak trees is dominated by precipitation patterns. El Niño events are linked to drought conditions over the IMC coinciding with increased $\delta^{18}\text{O}$ values in the tree-ring proxy (Figs. 2, 3). The opposite occurs during La Niña events.

The PDFs illustrate a clear WP El Niño and a less strong La Niña signal, with really dry years linked to WP El Niños. In contrast, no clear CT El Niño signal is preserved in the $\delta^{18}\text{O}_{\text{TR}}$ record, as indicated by the bimodality in the corresponding PDF. The different seasonal rainfall signals (wet and dry season rainfall) in the $\delta^{18}\text{O}_{\text{TR}}$ record are damped in the annually resolved proxy due to seasonally alternating isotope signatures in $\delta^{18}\text{O}$ of precipitation (Schollaen et al., 2013). Thus, CT El Niño signals seem to be obscured when followed by a La Niña event. This is the case for the strong CT El Niño event in 1982/83 that was followed by a La Niña, resulting in a low $\delta^{18}\text{O}_{\text{TR}}$ value (Fig. 2b, c). High-resolution intra-annual $\delta^{18}\text{O}_{\text{TR}}$ analyses help to disentangle the contrasting isotope effects of dry and rainy season rainfall patterns, as demonstrated in Schollaen et al. (2014). We conclude that the annually resolved tree-ring proxy is suitable for distinguishing between WP El Niño and La Niña, but not for CT El Niños. Correlation tests (Table 2) with a standard ENSO index (such as NINO3.4) show no correlation with the tree-ring record, as this index captures mixed signals from both ENSO flavors. Overall, the strongest and

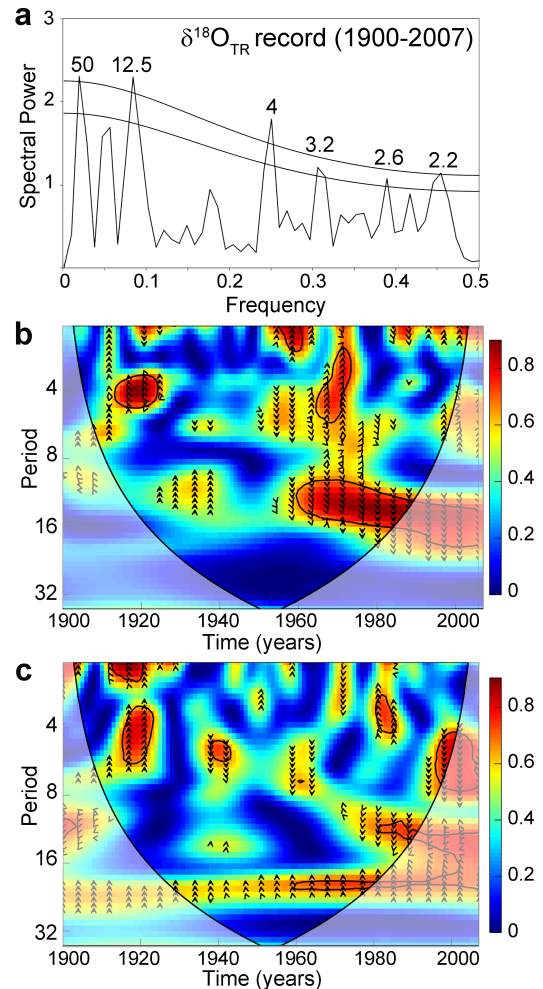


Figure 4. (a) Spectral analysis (Schulz and Mudelsee, 2002) of the $\delta^{18}\text{O}_{\text{TR}}$ chronology from 1900–2007. 90 and 95 % confidence levels are indicated. (b) Wavelet coherence transform comparing shared variance as a function of frequency between $\delta^{18}\text{O}_{\text{TR}}$ record and Warm Pool (WP) ENSO index (Jan_{n+1}) and (c) Cold Tongue (CT) ENSO index (Jan_{n+1}) for 1900–2007. The wavelet coherence illustrating temporal frequency coherence between the time series at given periods. The thick black contour designates where time series share significant coherence ($p = 95\%$) and the cone of influence where edge effects might distort the picture is shown as a lighter shade. Arrows indicate the phase relationship between series with in-phase pointing right and antiphase pointing left.

most significant ENSO signal in the tree-ring proxy data is that of WP El Niño.

Our analysis shows that the teleconnections described above are not stationary (Figs. 2, 4). There is a drop in correlation in the first half of the 20th century. Land use change is not an influencing factor as this study site is a very old forest and for the last few decades, a protected area. One can speculate this weakening teleconnection is related to the pattern of relatively weak and irregular ENSO activity in the middle of the 20th century (Tudhope et al., 2001). Arguably, there may

be other factors (e.g., Indian Ocean Dipole Mode) determining wetter or drier conditions in this period and the ENSO phenomenon may play a secondary role. In recent decades, a climate regime transition has preceded periods of strong and sustained ENSO events (e.g., O’Kane et al., 2014), leading to a stronger ENSO fingerprint in the $\delta^{18}\text{O}_{\text{TR}}$ record. Furthermore, Chang et al. (2004) reveal an interdecadal trend of increasing correlations between Indonesian monsoon rainfall and ENSO beginning in the late 1970s.

The $\delta^{18}\text{O}_{\text{TR}}$ record is a rainfall indicator for wet and dry season rainfall, albeit largely dominated by the wet season signal (Schollaen et al., 2013). Note that the “amount effect” leads to different isotopic signatures in $\delta^{18}\text{O}_{\text{TR}}$ values during wet and dry season. Thus, the dry season rainfall signal, which tends to have the highest coherence with ENSO, is damped in the annually resolved $\delta^{18}\text{O}_{\text{TR}}$ record by the following wet season signal. This may explain the low correlation between the tree-ring proxy and June to November ENSO indices. To distinguish the causes of inter-annual rainfall variability across Java future work needs to focus on high-resolution $\delta^{18}\text{O}_{\text{TR}}$ records.

5 Conclusions

In this study we used a $\delta^{18}\text{O}_{\text{TR}}$ chronology from teak (*Tectona grandis*) that correlates significantly with regional precipitation over Java (Schollaen et al., 2013) to examine various manifestations of ENSO. This is the first time a high-resolution $\delta^{18}\text{O}_{\text{TR}}$ record is used to detect signals of ENSO flavors in palaeoclimatic data as argued by Karamperidou et al. (2015). These results indicate the potential for generating reconstructions of different ENSO flavors from high-resolution intra-annual $\delta^{18}\text{O}$ records from appropriately selected regions, such as Java. Such palaeoclimatic records may help answer the many remaining questions surrounding the diversity of ENSO activity and past ENSO variability. In addition, the conclusions of our study call for caution when attempting to interpret proxy records using ENSO indices that are not able to distinguish between the two flavors (e.g., single standard indices such as NINO3.4). As shown here, single ENSO indices may capture mixed signals from both flavors, resulting in lower correlations with proxies and thus confounding paleoclimate reconstruction attempts. Furthermore, performing model-proxy comparisons using single ENSO indices may be misleading. For example, in multi-proxy reconstructions where proxies from different regions can be synthesized to reconstruct past ENSO variability it is important to account for the distinct (and often of opposite sign) influence of two flavors: convoluting their signals by using a single ENSO index can lead to potential misinterpretation of significant changes in past ENSO variability, as in the case of mid-Holocene (6 ka BP) coral proxies from the central Pacific (Karamperidou et al., 2015).

Lastly, our study calls for more emphasis on sampling long-term terrestrial $\delta^{18}\text{O}_{\text{TR}}$ records at seasonal and monthly resolution from selected regions such as northern or eastern Indonesia. Such high-resolution terrestrial $\delta^{18}\text{O}_{\text{TR}}$ records may have stronger correlations with ENSO flavors, and thus be appropriate for robust reconstructions of wet and dry season rainfall and of past variability of the two ENSO flavors.

Acknowledgements. We acknowledge the Bolin Centre’s, Climate Research Summer School during which this project and collaboration was conceived. We also thank two anonymous reviewers who provided excellent suggestions that improved the paper. Karina Schollaen was funded by the HIMPAC (HE 3089/4-1) and the CADY (BMBF, 03G0813H) project. Isotope analyses were funded by a Joint DFG/FAPESP Research Grant (HE3089/5-1). Christina Karamperidou is funded by NSF Award 1304910. Lamont-Doherty Earth Observatory contribution number 7935.

The article processing charges for this open-access publication were covered by a Research Centre of the Helmholtz Association.

Edited by: N. Abram

References

- Abram, N. J., Gagan, M. K., Cole, J. E., Hantoro, W. S., and Mudelsee, M.: Recent intensification of tropical climate variability in the Indian Ocean, *Nature Geosci.*, 1, 849–853, 2008.
- Adler, R. F., Huffman, G. J., Chang, A., Ferraro, R., Xie, P.-P., Janowiak, J., Rudolf, B., Schneider, U., Curtis, S., Bolvin, D., Gruber, A., Susskind, J., Arkin, P., and Nelkin, E.: The Version-2 Global Precipitation Climatology Project (GPCP) Monthly Precipitation Analysis (1979–Present), *J. Hydrometeorol.*, 4, 1147–1167, 2003.
- Aldrian, E. and Susanto, R. D.: Identification of three dominant rainfall regions within Indonesia and their relationship to sea surface temperature, *Int. J. Climatol.*, 23, 1435–1452, 2003.
- Aldrian, E., Dümenil Gates, L., and Widodo, F. H.: Seasonal variability of Indonesian rainfall in ECHAM4 simulations and in the reanalyses: The role of ENSO, *Theor. Appl. Climatol.*, 87, 41–59, 2007.
- Allan, J. R.: ENSO and Climatic Variability in the Past 150 Years, in: *El Niño and the Southern Oscillation: Multiscale Variability and Global and Regional Impacts*, edited by: Diaz, H. F. and Markgraf, V., Cambridge University Press, 3–56, 2000.
- Araguás-Araguás, L., Froehlich, K., and Rozanski, K.: Deuterium and oxygen-18 isotope composition of precipitation and atmospheric moisture, *Hydrol. Proc.*, 14, 1341–1355, 2000.
- Ashok, K. and Yamagata, T.: Climate change: The El Niño with a difference, *Nature*, 461, 481–484, 2009.
- Ashok, K., Behera, S. K., Rao, S. A., Weng, H., and Yamagata, T.: El Niño Modoki and its possible teleconnection, *J. Geophys. Res.-Oc.*, 112, C11007, doi:10.1038/461481a, 2007.
- Barbour, M. M.: Stable oxygen isotope composition of plant tissue: a review, *Funct. Plant Biol.*, 34, 83–94, 2007.

- Braganza, K., Gergis, J. L., Power, S. B., Risbey, J. S., and Fowler, A. M.: A multiproxy index of the El Niño–Southern Oscillation, A.D. 1525–1982, *J. Geophys. Res.-Atmos.*, 114, D05106, doi:10.1029/2008JD010896, 2009.
- Brienen, R. J. W., Helle, G., Pons, T. L., Guyot, J. L., and Gloor, M.: Oxygen isotopes in tree rings are a good proxy for Amazon precipitation and El Niño–Southern Oscillation variability, *Proc. Natl. Acad. Sci.*, 109, 16957–16962, 2012.
- Chang, C. P., Wang, Z., Ju, J., and Li, T.: On the Relationship between Western Maritime Continent Monsoon Rainfall and ENSO during Northern Winter, *J. Climate*, 17, 665–672, 2004.
- Charles, C. D., Cobb, K., Moore, M. D., and Fairbanks, R. G.: Monsoon–tropical ocean interaction in a network of coral records spanning the 20th century, *Mar. Geol.*, 201, 207–222, 2003.
- Clement, A. C., Seager, R., and Murtugudde, R.: Why Are There Tropical Warm Pools?, *J. Climate*, 18, 5294–5311, 2005.
- Cobb, K. M., Westphal, N., Sayani, H. R., Watson, J. T., Di Lorenzo, E., Cheng, H., Edwards, R. L., and Charles, C. D.: Highly Variable El Niño–Southern Oscillation Throughout the Holocene, *Science*, 339, 67–70, 2013.
- Collins, M., An, S.-I., Cai, W., Ganachaud, A., Guilyardi, E., Jin, F.-F., Jochum, M., Lengaigne, M., Power, S., Timmermann, A., Vecchi, G., and Wittenberg, A.: The impact of global warming on the tropical Pacific Ocean and El Niño, *Nature Geosci.*, 3, 391–397, 2010.
- Cook, E. R., D’Arrigo, R. D., and Mann, M. E.: A Well-Verified, Multiproxy Reconstruction of the Winter North Atlantic Oscillation Index since A.D. 1400*, *J. Climate*, 15, 1754–1764, 2002.
- Cook, E. R., Palmer, J. G., Ahmed, M., Woodhouse, C. A., Fenwick, P., Zafar, M. U., Wahab, M., and Khan, N.: Five centuries of Upper Indus River flow from tree rings, *J. Hydrol.*, 486, 365–375, 2013.
- Coster, C.: Zur Anatomie und Physiologie der Zuwachszonen- und Jahresringbildung in den Tropen, *Ann. Jard. Bot. Buitenzong*, 37, 49–160, 1927.
- Coster, C.: Zur Anatomie und Physiologie der Zuwachszonen- und Jahresringbildung in den Tropen, *Ann. Jard. Bot. Buitenzong*, 38, 1–114, 1928.
- D’Arrigo, R., Cook, E. R., Wilson, R. J., Allan, R., and Mann, M. E.: On the variability of ENSO over the past six centuries, *Geophys. Res. Lett.*, 32, L03711, doi:10.1029/2004gl022055, 2005.
- D’Arrigo, R., Wilson, R., Palmer, J., Krusic, P., Curtis, A., Sakulich, J., Bijaksana, S., Zulaikah, S., Ngkoimani, L. O., and Tudhope, A.: The reconstructed Indonesian warm pool sea surface temperatures from tree rings and corals: Linkages to Asian monsoon drought and El Niño–Southern Oscillation, *Paleoceanography*, 21, PA3005, doi:10.1029/2005pa001256, 2006.
- Emile-Geay, J., Cobb, K. M., Mann, M. E., and Wittenberg, A. T.: Estimating Central Equatorial Pacific SST Variability over the Past Millennium. Part II: Reconstructions and Implications, *J. Climate*, 26, 2329–2352, 2013.
- Evans, M. N., Kaplan, A., and Cane, M. A.: Pacific sea surface temperature field reconstruction from coral $\delta^{18}\text{O}$ data using reduced space objective analysis, *Paleoceanography*, 17, 7-1–7-13, 2002.
- Fowler, A. M., Boswijk, G., Lorrey, A. M., Gergis, J., Pirie, M., McCloskey, S. P. J., Palmer, J. G., and Wunder, J.: Multi-centennial tree-ring record of ENSO-related activity in New Zealand, *Nature Clim. Change*, 2, 172–176, 2012.
- Geiger, F.: Anatomische Untersuchungen über die Jahresringbildung von *Tectona grandis*, in: *Jahrbücher für wissenschaftliche Botanik*, edited by: Pfeffer, W., 1–658, 1915.
- Grinsted, A., Moore, J. C., and Jevrejeva, S.: Application of the cross wavelet transform and wavelet coherence to geophysical time series, *Nonlin. Processes Geophys.*, 11, 561–566, doi:10.5194/npg-11-561-2004, 2004.
- Haylock, M. and McBride, J.: Spatial Coherence and Predictability of Indonesian Wet Season Rainfall, *J. Climate*, 14, 3882–3887, 2001.
- Hendon, H. H.: Indonesian Rainfall Variability: Impacts of ENSO and Local Air-Sea Interaction, *J. Climate*, 16, 1775–1790, 2003.
- Jourdain, N., Gupta, A., Taschetto, A., Ummenhofer, C., Moise, A., and Ashok, K.: The Indo-Australian monsoon and its relationship to ENSO and IOD in reanalysis data and the CMIP3/CMIP5 simulations, *Clim. Dynam.*, 41, 3073–3102, 2013.
- Kao, H.-Y. and Yu, J.-Y.: Contrasting Eastern-Pacific and Central-Pacific Types of ENSO, *J. Climate*, 22, 615–632, 2009.
- Kaplan, A., Cane, M., Kushnir, Y., Clement, A., Blumenthal, M., and Rajagopalan, B.: Analyses of global sea surface temperature 1856–1991, *J. Geophys. Res.-Oc.*, 103, 18567–18589, 1998.
- Karamperidou, C., Di Nezio, P. N., Timmermann, A., Jin, F.-F., and Cobb, K. M.: The response of ENSO flavors to mid-Holocene climate: Implications for proxy interpretation, *Paleoceanography*, 30, 527–547, 2015.
- Kug, J.-S. and Ham, Y.-G.: Are there two types of La Nina?, *Geophys. Res. Lett.*, 38, L16704, doi:10.1029/2011GL048237, 2011.
- Kug, J.-S., Jin, F.-F., and An, S.-I.: Two Types of El Niño Events: Cold Tongue El Niño and Warm Pool El Niño, *J. Climate*, 22, 1499–1515, 2009.
- Kumar, K. K., Rajagopalan, B., Hoerling, M., Bates, G., and Cane, M.: Unraveling the Mystery of Indian Monsoon Failure During El Niño, *Science*, 314, 115–119, 2006.
- Larkin, N. K. and Harrison, D. E.: On the definition of El Niño and associated seasonal average U.S. weather anomalies, *Geophys. Res. Lett.*, 32, L13705, doi:10.1029/2005GL022738, 2005.
- Lau, N.-C. and Nath, M. J.: Impact of ENSO on the Variability of the Asian–Australian Monsoons as Simulated in GCM Experiments, *J. Climate*, 13, 4287–4309, 2000.
- Lee, T. and McPhaden, M. J.: Increasing intensity of El Niño in the central-equatorial Pacific, *Geophys. Res. Lett.*, 37, L14603, doi:10.1029/2010gl044007, 2010.
- Linsley, B. K., Wellington, G. M., Schrag, D. P., Ren, L., Salinger, M. J., and Tudhope, A. W.: Geochemical evidence from corals for changes in the amplitude and spatial pattern of South Pacific interdecadal climate variability over the last 300 years, *Clim. Dynam.*, 22, 1–11, 2004.
- Mann, M. E., Gille, E., Overpeck, J., Gross, W., Bradley, R. S., Keimig, F. T., and Hughes, M. K.: Global Temperature Patterns in Past Centuries: An Interactive Presentation, *Earth Interact.*, 4, 1–29, 2000.
- McCarroll, D. and Loader, N. J.: Stable isotopes in tree rings, *Quaternary Sci. Rev.*, 23, 771–801, 2004.
- McPhaden, M. J., Lee, T., and McClurg, D.: El Niño and its relationship to changing background conditions in the tropical Pacific Ocean, *Geophys. Res. Lett.*, 38, L15709, doi:10.1029/2011GL048275, 2011.

- Newman, M., Shin, S.-I., and Alexander, M. A.: Natural variation in ENSO flavors, *Geophys. Res. Lett.*, 38, L14705, doi:10.1029/2011GL047658, 2011.
- O’Kane, T. J., Matear, R. J., Chamberlain, M. A., and Oke, P. R.: ENSO regimes and the late 1970’s climate shift: The role of synoptic weather and South Pacific ocean spiciness, *J. Comput. Phys.*, 271, 19–38, 2014.
- Pfeiffer, M., Dullo, W.-C., Zinke, J., and Garbe-Schönberg, D.: Three monthly coral Sr/Ca records from the Chagos Archipelago covering the period of 1950–1995 A.D.: reproducibility and implications for quantitative reconstructions of sea surface temperature variations, *Int. J. Earth Sci.*, 98, 53–66, 2009.
- Pierrehumbert, R. T.: Thermostats, Radiator Fins, and the Local Runaway Greenhouse, *J. Atmos. Sci.*, 52, 1784–1806, 1995.
- Quinn, T. M., Taylor, F. W., and Crowley, T. J.: Coral-based climate variability in the Western Pacific Warm Pool since 1867, *J. Geophys. Res.-Oc.*, 111, C11006, doi:10.1029/2005JC003243, 2006.
- Ren, H.-L. and Jin, F.-F.: Niño indices for two types of ENSO, *Geophys. Res. Lett.*, 38, L04704, doi:10.1029/2010GL046031, 2011.
- Sano, M., Xu, C., and Nakatsuka, T.: A 300-year Vietnam hydroclimate and ENSO variability record reconstructed from tree ring $\delta^{18}\text{O}$, *J. Geophys. Res.*, 117, D12115, doi:10.1029/2012jd017749, 2012.
- Sarachik, E. S. and Cane, M. A.: *The El Niño-Southern Oscillation Phenomenon*, Cambridge University Press, London, 2010.
- Schollaen, K., Heinrich, I., Neuwirth, B., Krusic, P. J., D’Arrigo, R. D., Karyanto, O., and Helle, G.: Multiple tree-ring chronologies (ring width, $\delta^{13}\text{C}$ and $\delta^{18}\text{O}$) reveal dry and rainy season signals of rainfall in Indonesia, *Quaternary Sci. Rev.*, 73, 170–181, 2013.
- Schollaen, K., Heinrich, I., and Helle, G.: UV-laser-based microscopic dissection of tree rings – a novel sampling tool for $\delta^{13}\text{C}$ and $\delta^{18}\text{O}$ studies, *New Phytol.*, 201, 1045–1055, 2014.
- Schulman, E.: *Dendroclimatic Change in Semiarid America*, University of Arizona Press, Tuscon, Arizona, 1956.
- Schulz, M. and Mudelsee, M.: REDFIT: estimating red-noise spectra directly from unevenly spaced paleoclimatic time series, *Comput. Geosci.*, 28, 421–426, 2002.
- Stahle, D. W., Cleaveland, M. K., Therrell, M. D., Gay, D. A., D’Arrigo, R. D., Krusic, P. J., Cook, E. R., Allan, R. J., Cole, J. E., Dunbar, R. B., Moore, M. D., Stokes, M. A., Burns, B. T., Villanueva-Diaz, J., and Thompson, L. G.: Experimental Dendroclimatic Reconstruction of the Southern Oscillation, *Bull. Am. Meteorol. Soc.*, 79, 2137–2152, 1998.
- Takahashi, K., Montecinos, A., Goubanova, K., and Dewitte, B.: ENSO regimes: Reinterpreting the canonical and Modoki El Niño, *Geophys. Res. Lett.*, 38, L10704, doi:10.1029/2011GL047364, 2011.
- Taschetto, A. S. and England, M. H.: El Niño Modoki impacts on Australian rainfall, *J. Climate*, 22, 3167–3174, 2009.
- Torrence, C. and Compo, G. P.: A Practical Guide to Wavelet Analysis, *Bull. Am. Meteorol. Soc.*, 79, 61–78, 1998.
- Tudhope, A. W., Chilcott, C. P., McCulloch, M. T., Cook, E. R., Chappell, J., Ellam, R. M., Lea, D. W., Lough, J. M., and Shimmield, G. B.: Variability in the El Niño – Southern oscillation through a glacial-interglacial cycle, *Science*, 291, 1511–1517, 2001.
- Visser, H. and Molenaar, J.: Kalman Filter Analysis in Dendroclimatology, *Biometrics*, 44, 929–940, 1988.
- Wheeler, M. C. and McBride, J. L.: Australian-Indonesian monsoon. In: *Intraseasonal Variability in the Atmosphere-Ocean Climate System*, Springer Praxis Books, Springer Berlin Heidelberg, 2005.
- Wilson, R., Cook, E., D’Arrigo, R., Riedwyl, N., Evans, M. N., Tudhope, A., and Allan, R.: Reconstructing ENSO: the influence of method, proxy data, climate forcing and teleconnections, *J. Quat. Sci.*, 25, 62–78, 2010.
- Wilson, R., Miles, D., Loader, N., Melvin, T., Cunningham, L., Cooper, R., and Briffa, K.: A millennial long March–July precipitation reconstruction for southern-central England, *Clim. Dynam.*, 40, 997–1017, 2013.
- Wilson, R., Tudhope, A., Brohan, P., Briffa, K., Osborn, T., and Tett, S.: Two-hundred-fifty years of reconstructed and modeled tropical temperatures, *J. Geophys. Res.-Oc.*, 111, C10007, doi:10.1029/2005JC003188, 2006.
- Yeh, S.-W., Kug, J.-S., Dewitte, B., Kwon, M.-H., Kirtman, B. P., and Jin, F.-F.: El Niño in a changing climate, *Nature*, 461, 511–514, 2009.
- Zhu, M., Stott, L., Buckley, B., Yoshimura, K., and Ra, K.: Indo-Pacific Warm Pool convection and ENSO since 1867 derived from Cambodian pine tree cellulose oxygen isotopes, *J. Geophys. Res.*, 117, D11307, doi:10.1029/2011jd017198, 2012.